2013 IEEE/RSJ International Conference on
Intelligent Robots and Systems (IROS)
November 3-7, 2013. Tokyo, Japan

Rapid Turning at High-Speed: Inspirations from the Cheetah's Tail

Amir Patel*, *Student Member, IEEE* and M. Braae*, *Member, IEEE*

***Abstract*— Inspired by the cheetah, we present a novel tail control system for manoeuvring terrestrial robots at high speed. The mathematic model for a high-speed turn is derived and the model with a tail is shown to be more successful at rapid turns in simulation. We then built a high speed mobile platform with an actuated tail to experimentally validate the control algorithms. Further controller development is performed based on results of the initial simulations. Finally, we show that by rapidly swinging the tail, our system is capable of turning at much higher speeds than a tail-less version.**

I. Introduction

When one compares the manoeuvrability of animals to those of robots; robots most definitely fall short. No animal epitomizes this more than the cheetah (*Acinonyx jubatus*). Consider a cheetah in high-speed pursuit of its prey: the animal will rapidly re-adjust its trajectory in response to the evasive manoeuvres of the prey. It is this rapid, sensory driven feedback which future robots will need to harness for robust high speed locomotion.

Manoeuvrability can be defined as an animal's ability to change its velocity vector for a specific purpose as per the Biomechanics literature [1] [2]. This can be seen as increasing or decreasing the velocity vector magnitude (acceleration and deceleration) or changing its direction (turning). However, as stated by Alexander, when compared to steady locomotion, the biomechanics research of manoeuvrability has been very limited [3]. This can be attributed to the non-steady dynamics associated with these transient manoeuvres. Nevertheless, some exceptional contributions have been made by [4] [5] [6] [7].

Quadruped robot designs have also not focused on agility and manoeuvrability as discussed by Bowling [8]. As such, steady state motions such as bounding, trotting and galloping have been successfully implemented by various researchers [9] [10] [11]. Indeed, Boston Dynamics [12] has designed a high-speed quadruped robot capable of reaching speeds of over 12 m/s. But here again, the design goal is attaining the fastest speed and not explicitly on manoeuvrability.

The research reported here was inspired by video footage and images of cheetahs in pursuit of prey [13]. In the videos and photos (Fig. 1) it is seen that even though the cheetah is moving at high-speed, it is able to turn rapidly in response to the prey's attempts at evasion. What is interesting is that it appears to be swinging its tail (in the roll axis) during the turning manoeuvres. We hypothesize that the tail is providing a reactive torque which counteracts the toppling moment caused by the centrifugal force.

Corresponding author: a.patel@uct.ac.za. *Department of Electrical Engineering, University of Cape Town, South Africa

Fig. 1. A cheetah performing a rapid turn. It can be seen that the tail swings over along the roll axis during the turn. Image courtesy of National Geographic [14].

The robotics community has recently seen a surge of interest into the notion of actuated tails. These tails have successfully been employed for attitude control during flight [15] [16]. Kohut et al. have also demonstrated turning at low-speeds on their legged robot [17]. Recently, researchers at MIT have also investigated a Cheetah-inspired tail [18] for attitude control during the airborne phase as well as disturbance rejection (at standstill). Lastly, Patel and Braae [19] have demonstrated that an actuated tail can increase the acceleration capability of quadruped robots.

As is evident, the majority of research of tails in robotics has focused on attitude control. Except for Kohut et al. [17] and Patel and Braae [19], the focus has not explicitly been manoeuvrability.

Fig. 2. *Dima*, the high speed actuated tail robot.

In what follows, this paper will investigate the use of an actuated tail for a rapid turn at high-speed. Firstly, in Section II, a mathematical model will be developed for the rapid turning manoeuvre. Here simple reduced-order models with and without a tail are compared. It is shown that by actuating the tail, one can increase the capture region, thus implying more aggressive manoeuvres are possible. Following this, in Section III, a robot test platform (see Fig. 2) is designed to experimentally validate the tail controller system. This section also details the tail actuator design. Subsequently, in Section IV, the tail controllers are designed for the robot platform and simulated. Section V then deals with the experimental testing on the robot platform. Finally, Section VI contains a discussion of the results from which conclusions are drawn.

II. Modelling The High Speed Turn

A. Equations of Motion

To examine the benefits that an actuated tail can provide a terrestrial robot (or animal) performing a high speed turn, we first need to understand the underlying mechanics. Accordingly, we will need an adequate mathematical model for this scenario to validate via simulation.

Consider a rigid body (viewed from behind) travelling at some forward velocity when it suddenly initiates a turn to the left. If the centrifugal force is large enough the body (animal or robot) will topple. The centrifugal force equation is given by the equation:

$$F_{cent} = m_b \frac{v^2}{R}, \tag{1}$$

with m_b the mass of the body, v the forward velocity of the body and R the turning radius. It is evident that with increased speed the centrifugal force will increase quadratically.

With the addition of a tail, the proposed model for this scenario is depicted in Fig. 3.

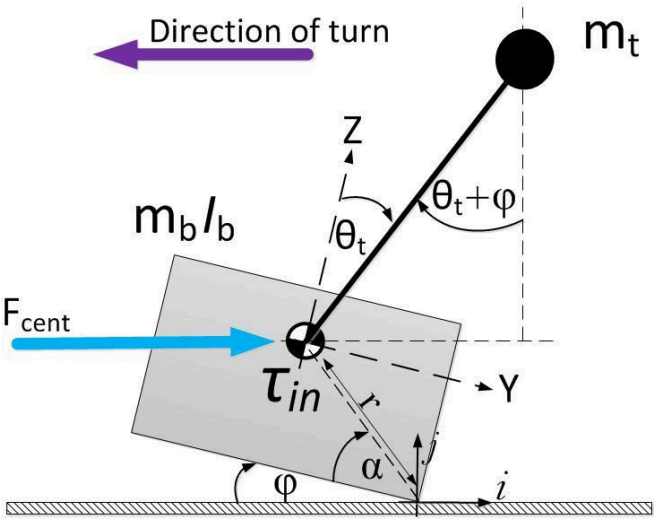

Fig. 3. The mathematical model for a high speed turning manoeuvre is illustrated graphically (viewed from behind). The model consists of a 2D rigid body and a point mass tail with a single point of contact with the ground.

The system can be modelled as a rigid body with one contact point on the outside of the turn similar to the model suggested for animals in chapter 3.5 of [20]. This situation will arise just before toppling when one wheel or leg is about to lift off the ground. Here we ignore the effects of slipping.

The tail is modelled as a point mass attached to an idealized massless rod of length L_t. Furthermore, the tail is actuated by an ideal torque actuator which is located at the centre of mass of the body much like that described in [18].

The system dynamics are modelled using the Euler-Lagrange method [21] [22] described by the equation[1]:

$$\boldsymbol{M(q)\ddot{q} + C(q,\dot{q})\dot{q} + G(q) = B\tau} \tag{2}$$

and the generalized coordinate vector is given by:

$$\boldsymbol{q} = [\varphi \quad \theta_t]^T. \tag{3}$$

Where, φ is the roll angle of the body and θ_t is the relative angle between the tail and body. Additionally, α and r are geometric properties of the body.

The centrifugal force can be seen as a generalized force [21] and is derived to be:

$$Q_\varphi = F_{cent}(r\sin(\varphi + \alpha)), \tag{4}$$

which directly effects the generalized coordinate φ.

Now that the system dynamics have been defined, the tail feedback control system can effectively be designed.

B. Tail Control System

If we reflect on the effect of the high speed turn, we can consider the centrifugal force to be a disturbance. In fact, this disturbance (if sufficiently large) will directly cause a net rolling moment, which will subsequently result in a roll rate and ultimately the robot toppling over. Hence, we desire to utilize the tail to counteract this effect.

It is decided to employ the tail as an actuator for a roll rate controller. This implies that the roll angle will not be regulated, which indicates that banked turns will be possible. This is different to the attitude controllers presented previously by [15] [16] [18].

Unfortunately, the system described in Section A, is an under-actuated system, which means we cannot employ Full State Feedback Linearization [23]. However, we can partially linearize one coordinate by using Partial Feedback Linearization (PFL) [24] on the body roll angle. The architecture for the control system is shown in Fig. 4:

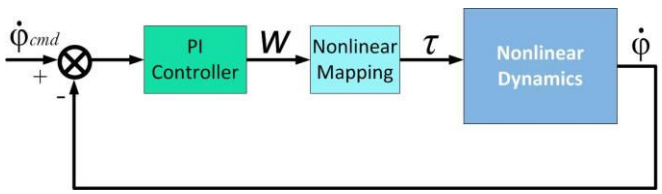

Fig. 4. Roll Rate Controller architecture

[1] For the sake of brevity, the ***M, B, C*** and ***G*** matrices have been omitted as their derivation is fairly trivial.

Following the method described in [24], we can linearize the roll angle by setting its second derivative to some variable 'w'. This results in the relationship:

$$\dot{\varphi} = \frac{w}{s} \tag{5}$$

which is now a linear system and 's' is the Laplace variable.

Now to map this linearized variable 'w' to the actual tail actuator torque, we can obtain the mapping:

$$\tau = L_t^2 m_t w - w(L_t^2 m_t + I_B) \tag{6}$$

The reader will note that the linearized dynamics are now simply that of an integrator with gain 'w'. We can then effortlessly design a PI controller, and place the two closed-loop poles anywhere we desire.

C. Simulation

The tail feedback control system is now tested in simulation and compared to that of the system without a tail.

Both configurations (body with and without control of the tail) are then simulated by varying initial body roll velocity and tail initial angle. The motive for this is that the centrifugal force will indeed induce a body roll rate and this will provide us with a measurement of comparative stability.

Additionally, the simulation will terminate once the body has come to rest, flipped over or the tail has reached the end of its swing.

The dynamic equations are modelled in Simulink using the model parameters depicted below in Table I. Furthermore, the roll rate controller dynamics are set to 4.5 rad/s with a damping factor of 0.8.

TABLE I. MODEL PARAMETERS

Parameter	Value
Body Mass ($\boldsymbol{m_b}$)	5 (kg)
Body Roll Inertia ($\boldsymbol{I_B}$)	0.093 (kgm^2)
Tail Mass ($\boldsymbol{m_t}$)	0.4 (kg)
Tail Length ($\boldsymbol{L_t}$)	0.5 (m)
Distance to centre of mass (r)	0.257 (m)
Angle to centre of mass ($\boldsymbol{\alpha}$)	0.897 (rad)

The phase portraits are shown in Fig. 5. It is clear that without the tail, the system has a limited basin of stability and does not return to zero for rates greater than 4.63 rad/s.

With the tail at zero initial angle (and its respective controller engaged), the roll rate is driven towards zero. Though, it is observed that the tail does not fully bring the body to rest.

With the tail at -90° initial value (facing into the turn), an improved disturbance rejection is shown. This is a very interesting result, as it is the same behaviour observed in the cheetah footage [14]. i.e. the cheetah first puts its tail into the direction of the turn before swinging it over.

However, the roll rate controller suffers from two issues:

- The controller is too slow to catch the disturbance in time. This implies that a feedforward torque is possibly required.
- At the end of the tail swing, the tail has a very high rotational velocity and as such would negate the effects of the roll stabilization once the swing is complete.

These two issues will need to be solved when the system is implemented on a physical system as discussed in the Section IV.

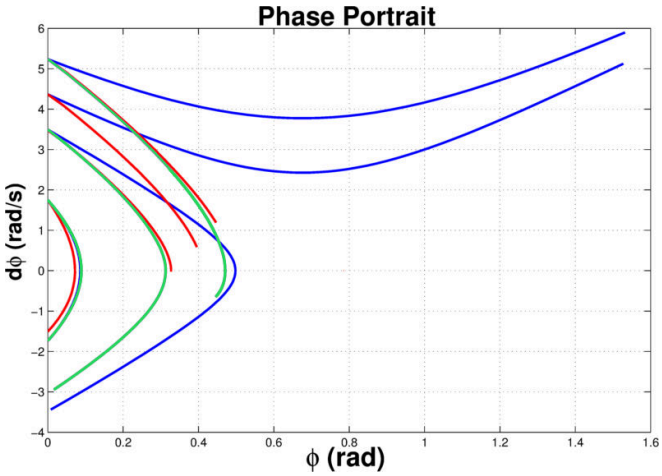

Fig. 5. Phase portrait comparing the system without tail (Blue plot), with tail at zero initial angle (Red plot) and with the tail at -90° initial angle (Green plot)

III. ROBOT DESIGN

The *Dima* robot (Fig. 2) was designed as a test platform for the actuated tail control system. The main design ideals were that we desired a high speed platform. We also required a platform with a high enough centre of gravity, so that it would indeed topple when performing rapid turns at high speed. This would ensure the results are applicable to not only wheeled robots but possibly also to legged robots.

A. Tail Design

Naturally, the tail design was of critical importance. The robot tail needed to match the performance (within reason) of the cheetah tail. Thus, we required a tail actuator with a high power as well as considerable length.

The tail rod was selected to be an aluminium rod of 10mm (mass of 99g) and the tail mass was chosen to be brass for its high density. This configuration would align closely with the massless rod assumption in in Section II.

The motor selected was the Maxon DCX-35L as it had a maximum continuous power rating of 120W and a relatively low mass. However, in order to select the optimal gear box ratio (N), we needed to determine the optimal tail mass as well, as detailed in [16].

Numerical simulations were then performed similar to those described in [15] [18]. Essentially, the model described in Section II, was used as a baseline with the tail in the 90° position and the body at 0°. The torque input (T) to the tail

was adapted from [18] to include the gear ratio (N) and provided as:

$$T = T_0 N\eta \left(1 - \frac{T_0 N\eta\omega}{4P^*}\right). \quad (7)$$

Where, T_0 is the motor's stall torque, η is the gearbox efficiency, ω is the shaft speed, and P^* is the maximum motor power. All these parameters were obtained from the manufacturer of the Maxon motor.

The simulation was run several times varying tail mass and gear ratio. The maximum body angular deflection was then captured and utilized as a performance metric. The reader should note that a tail length of 0.5 m (1 body length) and body mass of 5 kg were used in all simulation runs. The resulting plot is shown below in Fig. 6:

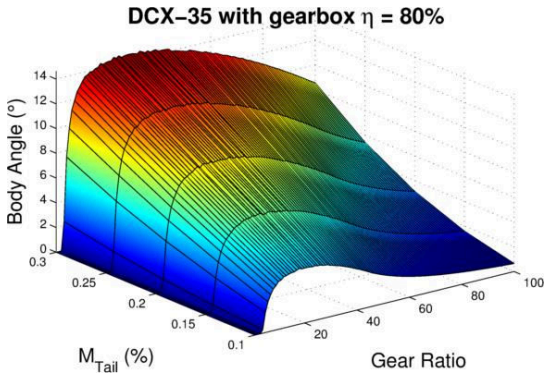

Fig. 6. The Maxon gearbox and tail mass selection plot is seen above. The body angle deflection was chosen as the performance metric which needed to be maximised.

The results suggest that for a tail mass of 10% body mass (0.5 kg), the gear ratio of 28 would be optimal. Thus, the closest Maxon gear box (26) was selected. However, due to supplier availability, only a 0.4 kg brass mass could be obtained at the time and as such was the selected value.

B. Mechanical Design

The Traxxas Stampede R/C car was selected as the base for the mechanical design. This car was chosen as it had a sufficiently high speed (+40 km/h) and also a high centre of gravity aligning with the model described in Section II.A.

Fig. 7. Solidworks model of Dima

The car was modelled in Solidworks as depicted in Fig. 7 and was majorly modified by the addition of the following:

- Two aluminium platforms for mounting of the on-board electronics
- Stiffer springs to accommodate the increased weight
- A roll cage to protect the electronics from impacts at high speed

C. Hardware and Software Design

The onboard processor was the STM32F4 Discovery with an ARM Cortex M4 running at 168 MHz. Logging was implemented on a micro-SD card. For telemetry an XBee Pro was selected and was used for communication between a host PC and the robot.

To drive the tail motor a Pololu 18V15 PWM motor controller was employed. In order to sense all the states (velocity, angular rates) as well as receive estimated attitude angles, the Tellumat SP1000GA was selected. Via its Extended Kalman Filter, the sensor provided state information updates at 50 Hz.

The software consisted of a FreeRTOS [25] kernel, which allowed multi-tasking capability with the added benefit of real time operation. Lastly, Second Order Butterworth filters were implemented on the raw data provided by the IMU.

IV. Dima Control System Design

The task was then to design the tail controller algorithms for the Dima robot platform to be tested experimentally. With insights gained in Section II-C a revised controller architecture was proposed and is illustrated in Fig. 8.

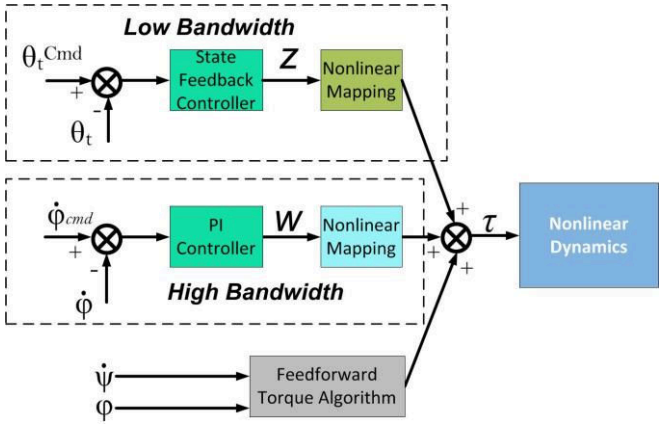

Fig. 8. Revised tail controller architecture.

The first addition to the architecture is a low bandwidth tail position controller which will serve a dual purpose. Firstly, it will slow down the tail appropriately once the turn is complete and the roll rate has been damped. Secondly, this controller will allow the tail to be placed in the correct initial position before a turn.

The Feedforward Torque Algorithm (FTA) will allow the tail system to automatically swing the tail by the delta torque induced by the turn. This will allow the tail to damp out the disturbance of the turn, leaving the roll rate controller to diminish any residual errors due to modelling inaccuracy.

A. Mathematical Model for Controller Design

To design the controllers effectively, we employed the model described in Section II and modified it for this particular robot. If we re-examine equation (1), we can see

that the centrifugal force is dependent on the turning radius (R). If we assume that the robot's steering mechanism is a True Ackermann Mechanism [26], the turning radius is given by:

$$R = \frac{L}{\tan(\delta)}. \tag{8}$$

Where δ is the steering angle and L is the length between the front and rear axles. For this specific robot L is 0.28 m.

Furthermore, the steering angle is not produced instantly and also has dynamics (due to the servo motor). Thus, these dynamics need to be factored in and induce a lag in the centrifugal force. For simplicity, we can model this as a first order dynamic system. After simple steering tests on the car, the time constant was determined to be 0.8 s for the steering transfer function.

With the exception of the servo model, the mathematical model employed will be the same as that of Section II. The reader should note that the model ignores the effect of the springs on the car and this could affect the experimental data. However, considering that the focus of the research is on the tail algorithms, this was deemed a feasible assumption.

B. Tail Position Controller Design

As discussed previously the tail position controller, will slow down the tail at the end of its swing and also allow command of the tail to the correct initial value.

Once more, PFL is utilized to linearize one coordinate. In this case, the tail angle acceleration is set to some variable 'z', which is then a linear system. The mapping from 'z' to actual torque is provided by:

$$\tau_{pos} = m_t z L_t^2 - g m_t L_t \sin\theta_t \tag{9}$$

Now that the dynamics are linearized, a full state feedback controller (with an additional integrator state) is designed to place the poles much slower than that of the rate controller. As such, the fasted pole is placed at 1 rad/s.

C. Feedforward Torque Algorithm (FTA)

The FTA will allow the tail to dampen out the disturbance much faster. This is achieved by first calculating the torque produced by the centrifugal force and then determining if this is greater than that of the gravitational torque. If this condition is true, it will directly command this 'delta torque' to the tail motor.

After some algebraic manipulation, the centrifugal force can be written as:

$$F_c = m_b v \dot{\psi} \tag{10}$$

Note, $\dot{\psi}$ is the yaw rate. The torque can be calculated as:

$$\tau_{cent} = F_{cent} r \sin(\alpha + \varphi). \tag{11}$$

Now, if this magnitude is greater than the torque induced by the gravity vector passing through the body's centre of mass, the value is directly commanded to the tail.

C. Simulation

The model and aforementioned controllers were then numerically simulated in Simulink. The system is given an initial steering angle of zero, and then stepped to 30°. After 0.5 s, to keep the tail angle within its range, the steering is again stepped back to zero, thereby ending the turn. This is done at varying initial forward velocity values.

The maximum initial velocity possible with the tail controller algorithms before toppling occurred was 4.5 m/s. The results are shown in Fig. 9. It is clear that the body angle is brought back to zero and furthermore that the tail velocity is sufficiently slow. This velocity resulted in 16.8 m/s^2 radial (lateral) acceleration to be experienced.

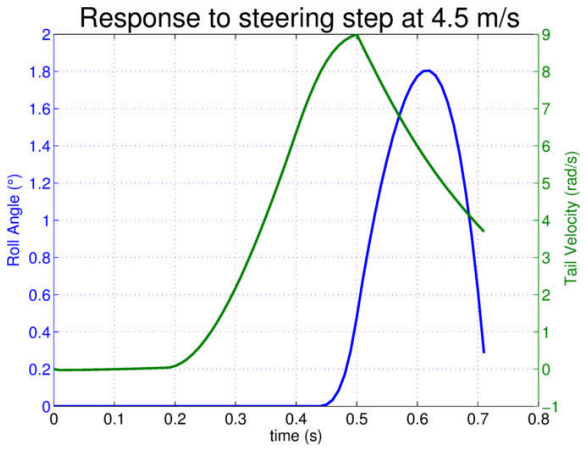

Fig. 9. Body angle and tail velocity responses to a 30° steering step (length 0.5 s) initiated at 4.5 m/s.

A model without a tail was also subjected to the centrifugal force and the maximum velocity a successful turn occurred at was at 2m/s.

V. Experiments

The effectiveness of the tail controller algorithms was evaluated on the Dima robot. The test results would indeed validate the motive for employing an actuated tail on a high speed robot.

The test procedure was as follows:

- The robot would drive straight until attaining steady state velocity
- The steering controller would engage a 30° steering angle for 0.5 s in the right direction
- After 0.5 s, the steering would return to zero

The performance metric was the lateral acceleration in the inertial frame which was derived from the IMU.

A. Results

The tail-less robot attained a greater velocity (~3.1 m/s) before toppling over during the turning step than the model in Section III predicted. The maximum lateral acceleration obtained was ~8.3 m/s^2 and is depicted in Fig. 10. The robot with the tail also performed better than the model predicted, and was capable of turning at 7.5 m/s and achieved ~11.8 m/s^2 lateral acceleration. The reader is encouraged to view the attached videos (See Supplementary Material).

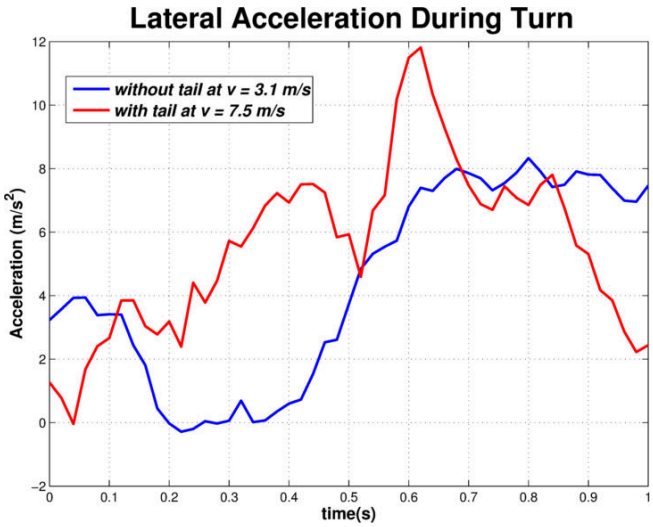

Fig. 10. Lateral acceleration obtained. With the tail controller, the robot was able to turn at a velocity of 7.5 m/s and achieve a maximum acceleration of ~11.8 m/s^2.

VI. Discussion and Conclusion

The system surpassed predicted velocity performance for both tailed and tail-less models. This can be attributed to the robot's springs which were not modelled. These allow the robot to perform a banked turn, which increases stability.

The lateral acceleration achieved with the tail was ~30% less than predicted and can be attributed to the tail not being fully aligned with the COM which would reduce the turning yaw rate. Nevertheless, the addition of the tail enabled the robot to still achieve a ~40% increase in lateral acceleration compared to the tail-less version.

This research has shown that actuated tails are indeed a viable solution to the question of manoeuvrability for future high speed terrestrial robots. Future work will involve investigation of two degree of freedom tails as it will allow torque to be generated in more axes.

Acknowledgment

The authors would like to gratefully acknowledge James Gowans, Justin Coetser and Javaad Patel for their technical support on the Dima robot. Also, A/Prof. Azeem Khan for support and Prof. Ed Boje for advice and contributions to the controller design.

References

[1] P. W. Webb, "Maneuverability - General Issues," *IEEE Journal of Oceanic Engineering,* vol. 29, no. 3, pp. 547-555, 2004.

[2] D. Jindrich and M. Qiao, "Maneuvers during legged locomotion," *Chaos,* vol. 19, 2009.

[3] R. M. Alexander, Principles of Animal Locomotion, Princeton University Press, 2006.

[4] D. Jindrich, N. Smith, K. Jespers and A. Wilson, "Mechanics of cutting maneuvers by ostriches," *The Journal of Experimental Biology,* vol. 210, pp. 1378-1390, 2007.

[5] C. Moreno, Biomechanics of non-steady locomotion: Bone loading, tunring mechanics and maneuvering performance in goats, Cambridge, Massachusetts: Harvard University, 2010.

[6] S. Williams, J. Usherwood, K. Jespers, A. Channon and A. Wilson, "Exploring the mechanical basis for acceleration: Pelvic limb locomotor function during accelerations in racing greyhounds (Canis familiaris)," *The Journal of Experimental Biology,* vol. 212, pp. 550-565, 2009.

[7] S. Williams, H. T, U. J.R, Wilson and A.M, "Pitch then power: Limitations to acceleration in quadrupeds," *Biology Letters,* vol. 5, pp. 610-613, 2009.

[8] A. Bowling, "Impact forces and agility in legged robot locomotion," *Journal of Vibration and Control,* vol. 17, no. 3, pp. 335-346, 2010.

[9] H. Kazemi, V. Majd and M. Moghaddam, "Modeling and robust backstepping control of an underactuated quadruped robot in bounding motion," *Robotica,* pp. 1-17, 2012.

[10] D. Krasny and D. Orin, "Evolution of Dynamic Maneuvers in a 3D Galloping Robot," in *IEEE International Conference on Robotics and Automation*, Orlando, Florida, 2006.

[11] X. Wang, M. Li, P. Wang and L. Sun, "Running and Turning Control of a Quadruped Robot with Compliant Legs in Bounding Gait," in *IEEE International Conference on Robotics and Automation*, Shanghai, China, 2011.

[12] Boston Dynamics, "CHEETAH- Fastest Legged Robot," Boston Dynamics, 2012. [Online]. Available: http://www.bostondynamics.com/robot_cheetah.html. [Accessed 17 October 2012].

[13] National Geographic, "Big Cats Initiative: Big Cat Facts," National Geographic, 2012. [Online]. Available: http://animals.nationalgeographic.com/animals/big-cats/facts/. [Accessed 17 October 2012].

[14] National Geographic, "Cheetah (Acinonyx jubatus)," 2013. [Online]. Available: Cheetah Acinonyx jubatus. [Accessed 10 March 2012].

[15] E. Chang-Siu, T. Libby, M. Tomizuka and F. R.J, "A Lizard-Inspired Active Tail Enables Rapid Maneuvers and Dynamic Stabilization in a Terrestrial Robot," in *IEEE/RSJ International Conference on Intelligent Robots and Systems*, San Francisco, California, 2011.

[16] A. Johnson, T. Libby and E. Chang-Siu, "Tail Assisted Dynamic Self Righting," in *Proceedings of the Fifteenth International Conference on Climbing and Walking Robots and the Support Technologies for Mobile Machines*, Baltimore, MD, USA, 2012.

[17] N. Kohut, D. Haldane, D. Zarrouk and R. Fearing, "Effect of Inertial Tail on Yaw Rate of 45 gram Legged Robot," in *Proceedings of the Fifteenth International Conference on Climbing and Walking Robots and the Support Technlogies for Mobile Machines*, Baltimore, MD, USA, 2012.

[18] R. Briggs, J. Lee, M. Haberland and S. Kim, "Tails in Biomimetic Design: Analysis, Simulation and Experiment," in *IEEE/RSJ International Conference on Intelligent Robots and Systems*, Vilamoura, Algarve, Portugal, 2012.

[19] A. Patel and M. Braae, "An Actuated Tail Increases Rapid Acceleration Manoeuvres in Quadruped Robots," in *International Joint Conferences on Computer, Information, Systems Sciences and Engineering*, 2012.

[20] A. Biewener, "Maneuverability versus Stability," in *Animal Locomotion*, Oxford University Press, 2003, p. 58.

[21] D. Greenwood, Advanced Dynamics, Cambridge: Cambridge University Press, 2003.

[22] R. Murray, Z. Li and S. Sastry, A Mathematical Introduction to Robotic Manipulation, CRC Press, 1994.

[23] R. Tedrake, "Fully Actuated vs. Underactuated Systems (Course Notes)," MIT OpenCourseWare, 2009.

[24] A. Shkolnik and R. Tedrake, "High-Dimensional Underactuated Motion Planning via Task Space Control," in *IEEE International Conference on Intelligent Robots and Systems*, 2008.

[25] FreeRTOS, "FreeRTOS," 2013. [Online]. Available: http://www.freertos.org/.

[26] M. Sotelo, "Lateral Control Stratgy fo Autonmous Steering of Ackerman-like Vehicles," *Robotics and Autonomous Systems,* vol. 45, pp. 223-233, 2003.